Silicone-based Capacitive E-skin for Exteroception and Proprioception

Abu Bakar Dawood, Hareesh Godaba, Ahmad Ataka, and Kaspar Althoefer, *Senior Member, IEEE*

***Abstract*— Thin and imperceptible soft skins that can detect internal deformations as well as external forces, can go a long way to address perception and control challenges in soft robots. However, decoupling proprioceptive and exteroceptive stimuli is a challenging task. In this paper, we present a silicone-based, capacitive E-skin for exteroception and proprioception (SCEEP). This soft and stretchable sensor can perceive stretch as along with touch at 100 different points via its 100 tactels. In this paper, we present a novel algorithm that decouples global strain from local indentations due to external forces. The soft skin is 10.1cm in length and 10cm in width and can be used to accurately measure the global strain of up to 25% with an error of under 3%; while at the same time, can determine the amplitude and position of local indentations. This is a step towards a fully soft electronic skin that can act as a proprioceptive sensor to measure internal states while measuring external forces.**

I. Introduction

Conventional or rigid robots have been employed extensively in the industry; however, these robots lack compliance, adaptability and are not best suited for safe Human-Robot Interaction (HRI). Soft robots provide inherent compliance and safety being contenders for the challenges of robots interacting with humans and generally, operating in safety-critical environments [1]–[3].

Conventional robots can be controlled effectively by built-in feedback systems and analytical models. However, in soft robots, infinite degrees of freedom and compliance, makes it difficult to have an accurate feedback for achieving control.

In real environments, robots encounter different types of stimuli simultaneously [4]. Researchers have studied capacitive [5], [6], optical [7], [8], liquid-filled channels [9] and resistive [10], [11] methods for sensing internal strains in soft robots. Larson et al. employed electroluminescent soft capacitors molded into Ecoflex and examined the effects of stretch, pneumatic pressure and external force on capacitance individually [5]. However, the coupling or the response of capacitance owing to two or more stimuli acting simultaneously has not been studied extensively.

Different sensing techniques have been employed in combination, to sense more than one stimulus at the same time. Totaro et al. used a combination of resistance and piezoresistivity to determine bending and external force [12]. Thin tracks of gold nanoparticles were fabricated using supersonic cluster beam implantation, and bending was sensed by the change in resistance of these conductive tracks. The external force was measured by the change in intensity of light transmitted through photo waveguides. However, simpler manufacturing methods and their application in soft actuators are yet to be explored.

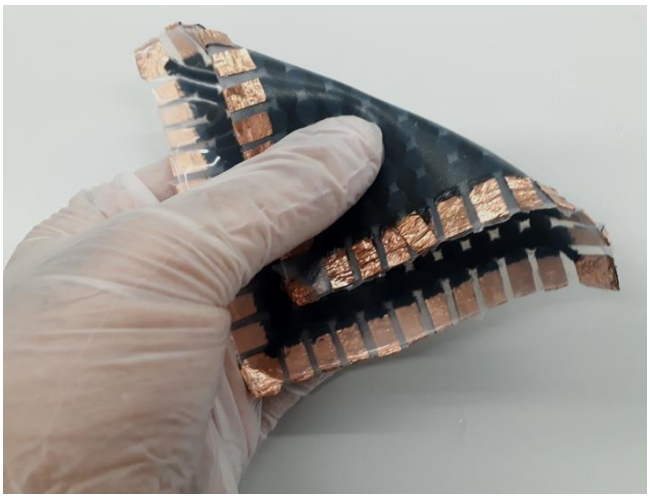

Figure 1: SCEEP, a silicon-based capacitive skin, is highly stretchable and foldable.

Tactile sensing is a well-researched area in the challenge towards equipping robots with the ability to sense touch. Touch sensors, combined with the added functionality of force sensing have been developed [13]. Similarly, soft touch and force sensors have been used at the fingertips of humanoid robots [14]. These fingertip sensors are not just vital in improving the grasping of random objects but enable them to hold finer objects like cloth and fabric [15]. Matsuno et al. used conductive fabric to utilize the change in capacitance for sensing proximity and touch and used it for safe Human-Robot Interaction (HRI) [16]. Maiolino et al. developed modular pressure sensors, that can be embedded with curved surfaces and can measure pressure. Their approach utilizes non-deformable capacitors for correcting sensor variations due to temperature changes [17], [18].

The Perception of multimodal stimuli is also an important capability that has been investigated. A graphene-based e-skin, to measure humidity and pressure was developed by Dong et al. [19]. In addition to this, the temperature was measured using the change in resistance of the graphene layer. Hua et al. have worked on a highly stretchable and multifunctional sensing skin [20]. Similar e-skins have layers of different sensing elements, making these capable of measuring multiple stimuli at the same time [21]–[23].

This work was supported by a research grant from the Engineering and Physical Sciences Research Council (EPSRC) in the framework of the, National Centre for Nuclear Robotics (NCNR) project (EP/R02572X/1).

A. Dawood, H. Godaba, A. Ataka and K. Althoefer are with the Centre for Advanced Robotics @ Queen Mary, Queen Mary University of London, London, E1 4NS, United Kingdom. (e-mail: a.dawood@qmul.ac.uk, h.godaba@qmul.ac.uk, a.rizqi@qmul.ac.uk, k.althoefer@qmul.ac.uk)

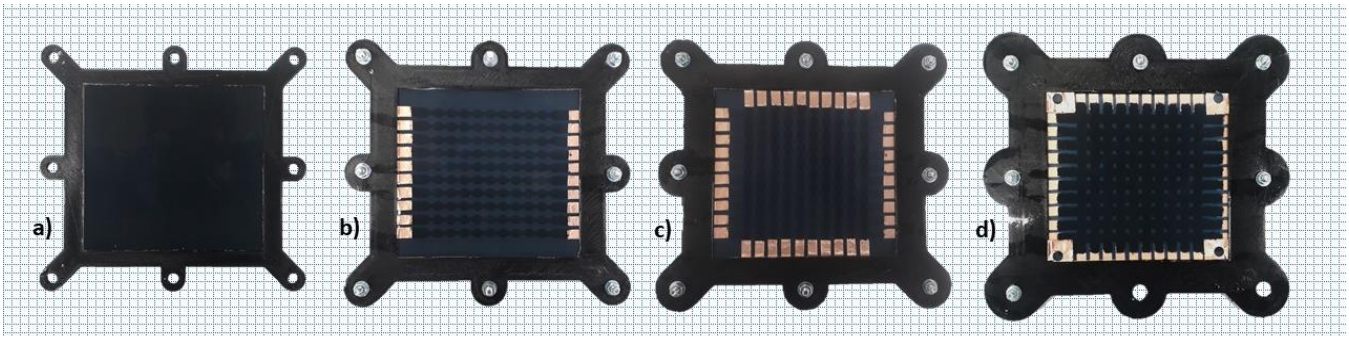

Figure 2: Four steps of fabricating SCEEP. a) shows the base layer of Ecoflex cured in the mold. b) shows the first set of interlocking terminals with a layer of Ecoflex cured on top of it. A copper tape was used as a connection between carbon grease terminals and external circuitry; c) shows the next set of interlocking terminals made perpendicular to the previous set; d) shows SCEEP just before the disassembly of the mold. The common ground layer, combination of both the electrode sets is shown with four copper tape terminals for the external connections.

However, detecting and decoupling different modes of mechanical stimuli, such as pressure, force, and strain, by utilizing a single sensing skin is an outstanding challenge in the domain of soft sensing. In this work, we develop a Silicone-based Capacitive E-skin for Exteroception and Proprioception (SCEEP) that uses a matrix of capacitive sensors and propose a decoupling algorithm that can calculate the global strain and identify the location of a local indentation at the same time.

Human beings have cutaneous receptors to detect touch and the amount of pressure applied [24]. In addition to these cutaneous receptors, we have mechanoreceptors in our muscles and joints that give kinesthetic or proprioceptive feedback to sense position and motion. The motivation for our work is to make a soft stretchable skin capable of multimodality just like human skin – an e-skin that can localize and quantify touch as well as the stretch that it experiences.

In our previous work, we studied both the individual and coupled effects of stretch, internal pressure and external force on a soft capacitive sensor [25]. In this paper, we have employed a capacitive sensor array to determine stretch and indentation. We used two sets of orthogonal terminals, at different heights from a common ground. The global change in capacitance of the terminals was used to determine stretch, while a local change in capacitance is interpreted as localized touch.

II. Methodology

A. Fabrication of the Molds

The mold for our sensor insulation layers was modeled in Creo Parametric, and then 3D printed using an Ultimaker3 rapid prototyping machine using polylactic acid (PLA). Each layer was fabricated using EcoFlex 00-50 that was poured in the printed layer molds.

B. Fabrication of the capacitive skin

We used Ecoflex 00-50 to fabricate the soft e-skin, because of the low cost, the ease of use and its biocompatibility. The terminals were made using carbon grease. Carbon grease can be applied easily and has a high stretchability. Stretching the carbon grease terminals results in a change of resistance of the carbon grease terminals. A copper tape of 0.07 mm thickness was used as a connection between the carbon grease electrodes and the external circuitry.

As a first step, both parts A and B of Ecoflex 00-50, mixed in equal ratios, were poured into the base plate; the layer thickness was maintained by levelling the Ecoflex material whilst being in its pre-cured state. Curing of Ecoflex was conducted at room temperature. It is noted that curing in an oven at higher temperatures may deform the PLA mold. After the bottom layer was cured, the first set of carbon grease terminals was created using a stencil with a thickness of 0.25 mm. For the terminal design, an interlocking design was adopted, as proposed by Lee et al. [26]; this pattern has been proven to have a better sensitivity when compared to rectangular patterns. After the stencil was removed, copper tape terminals of 6mm width and 20mm length were pasted on the top of the carbon grease terminals on both sides. Good electrical connectivity between copper terminals and carbon grease terminals was confirmed using an ohmmeter.

After the terminals were tested, a 3D printed plate of 0.5mm thickness was placed on top of the base plate and screwed to it, to avoid any leakage of Ecoflex. After that, Ecoflex was poured again into the mold and on top of the already cured first layer. The layer thickness was maintained by levelling the pre-cured Ecoflex mixture with a wooden stick, removing any excess.

After the second Ecoflex layer had been applied and cured, the stencil was placed orthogonally to the initial pattern (90 degrees with respect to the pattern of the base layer) on top to create the second set of carbon grease terminals. The same process was repeated, and after curing the third layer, a common ground terminal was printed. To print this ground terminal, the first stencil was placed on top of the third layer, and the terminals were printed. Then the second stencil was placed on top of these printed terminals and orthogonal terminals were printed, resulting in one terminal having an interlocking design. The copper tape terminals were placed at the four corners of the e-skin for the connection of the ground terminal with external circuitry. A final plate of 0.5 mm thickness was placed, and a final layer of Ecoflex was applied and cured. After disassembling the mold, the electrical connections were checked again. The resultant silicone-based capacitive skin has a thickness of 2 mm and is ready to be used for experimentation.

C. Experimental Setup

For the stretching of the sensor skin, an M8 lead screw with a SUNCOR stepper motor was used. The stepper motor

has a step angle of 1.8° and was controlled using a stepper driver (Big Easy stepper driver, by Sparkfun). The motor holder and all other components along with the skin holders were 3D printed. The skin holder was designed with cavities to accommodate male header pins. When the e-skin was clamped in the holder, these header pins, in contact with copper tape terminals, were used as electrical connections between the e-skin and the external circuitry.

For measuring the capacitance, an integrated circuit (IC) CAV 424 by Analog Microelectronics, was used. This capacitance-to-voltage converting integrated circuit (IC), compares the capacitance to a reference capacitance and converts the difference to voltage. The data was acquired by using one CAV424 in conjunction with two 16-1 multiplexers as shown in Fig. 3.

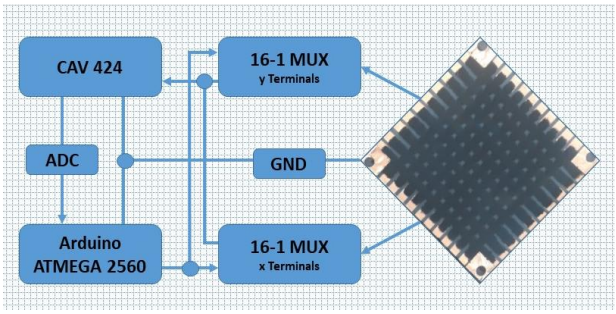

Figure 3: Flow chart for data acquisition. SCEEP is connected to the CAV 424 through two 16-1 multiplexers, one for the x-terminals and another for the y-terminals. The output of the CAV 424 is read at ADC of ATMEGA 2560.

The capacitance of each individual terminal and the ground was first measured by a bridge meter (HM8118 LCR bridge meter). It was found that the introduction of a multiplexer adds to the parasitic capacitance. Hence, the minimum capacitance measured through the multiplexer was used as the reference capacitance for the CAV424, i.e., 47pF. The operational frequency of the CAV424 oscillator was set to 5 kHz.

After setting the initial parameters, the CAV 424 was calibrated. The CAV 424 gives an output voltage that is a linear function of the reciprocal of the capacitance being measured. Hence, the minimum and maximum capacitance for the calibration of the CAV424 were selected such that the range of the capacitance of our e-skin is in the most sensitive region of the capacitance-voltage curve. Using trimmer resistors, the output voltage of the CAV424 was set to be 1V for 47pF and 4.3V for 220pF. The calibration curve for the CAV424 is shown in Fig. 4. A trendline of a 4th degree polynomial was used and to get an equation for the capacitance in terms of the voltage measured at the Analog to Digital Converter (ADC), the *x* and *y* data in the calibration curve was swapped.

An Arduino Atmega2560 microcontroller was used for switching the terminals using multiplexers and reading voltage signals at the ADC. The sensor values were later sent to a computer via a serial port. The stepper motor was also controlled by the Arduino, and the minimum distance for stretching and un-stretching of the skin was set to 6.25mm; this was achieved by five complete rotations of the motor shaft. The experimental setup is shown in Fig. 5.

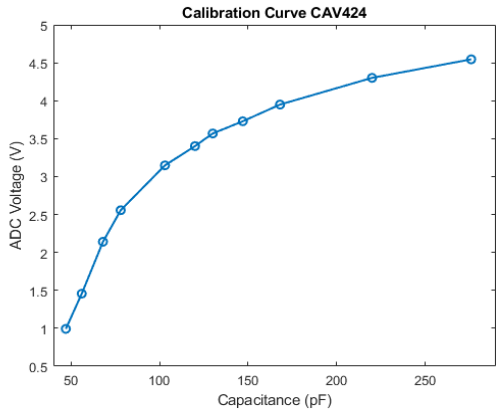

Figure 4: Calibration curve for CAV424 obtained by using standard capacitances connected through a multiplexer.

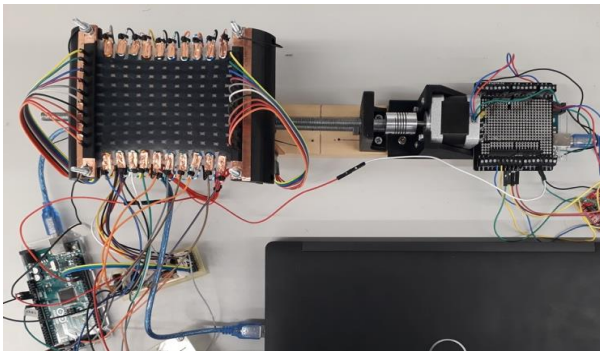

Figure 5: Complete experimental setup showing capacitive skin, mounted on the mechanism for stretching along with control circuitry.

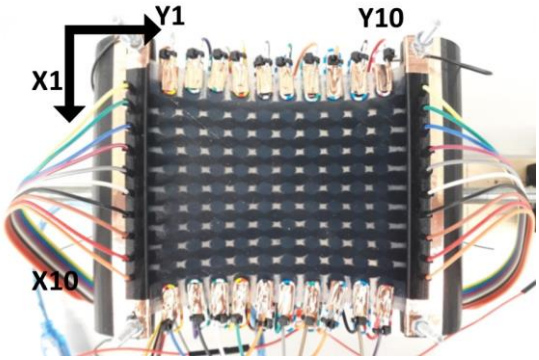

Figure 6: Nomenclature of terminals of SCEEP. The top left corner is taken as the origin.

III. The Decoupling Algorithm

The data acquired from SCEEP is then processed by our decoupling algorithm. This algorithm decouples stretch from indentation and quantifies both stimuli. For a better understanding of the algorithm, familiarization with the nomenclature of the SCEEP is important, Fig. 6. The top left corner was taken as the origin, and the clamped terminals were named X1, X2 to X10. Similarly, the terminals orthogonal to the direction of stretch were named Y1, Y2 to Y10. Both sides of the terminals were connected to each other and then to the input terminal of the CAV424 through a multiplexer.

The capacitance of each terminal with respect to the ground terminal was measured, resulting in a 2x10 matrix for each state. Fig. 7 shows the percentage difference in capaci-

tance with the initial states of terminals X1, X5, X6 and X10, when the skin is about to be stretched. Fig. 7 also shows the average capacitances of all terminals in different states. The SCEEP was stretched from 0 to 25mm with a step change of 6.25mm. The initial length of the skin was 101mm; hence, a maximum stretch or $\lambda = 1.2475$ was achieved. Here stretch is defined as the ratio of the final length to the initial length, $\lambda = L/L_o$

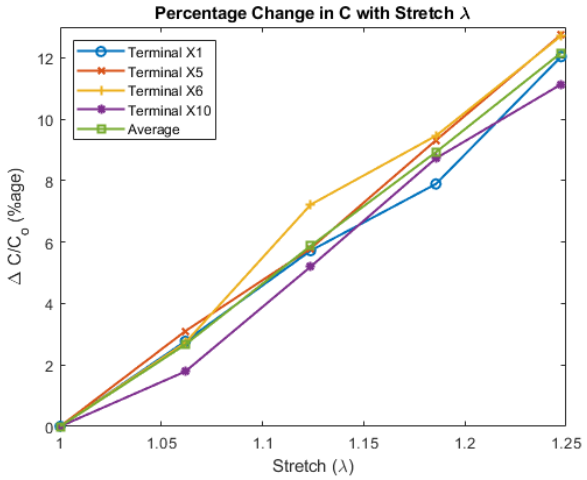

Figure 7: Percentage increase in capacitance of terminals X1, X5, X6, X10 and average of all X terminals with stretch.

To obtain a 10x10 matrix representing all the nodes of the skin, each X element of this 2x10 matrix was multiplied to all the Y elements individually to make a 10x10 matrix and Δ was calculated. We define $\Delta = \left(\frac{\sqrt{C_x C_y} - C_{0x} C_{0y}}{\sqrt{C_{0x} C_{0y}}}\right)$ where, $\boldsymbol{C_x}$ and $\boldsymbol{C_y}$ are the capacitances of the *x* and *y* terminals in a particular state while $\boldsymbol{C_{0x}}$ and $\boldsymbol{C_{0y}}$ are the capacitances of x and y terminals in its initial state. To achieve local indentation, an indenter with a circular tip of 5mm diameter was 3D printed. It was held in a multipurpose workstation (Dremel 220) and two indentation depths 5mm and 10mm from the zero states were fixed. For decoupling indentation and stretch, a MATLAB code was written; the corresponding flowchart is shown in Fig. 8.

After developing the node matrix and calculating Δ, the algorithm finds the maximum value in the node matrix and then determines the coordinate points of that maximum value. To calculate the stretch, the algorithm defines four reference points along the diagonal and selects two reference points at a maximum distance and at least two nodes away from the point of indentation. From those two selected nodes, the corresponding y-terminals were selected, and change in capacitance of those y-terminals with the initial state was used to calculate stretch. The mean stretch was calculated by taking the average of the stretch of both terminals.

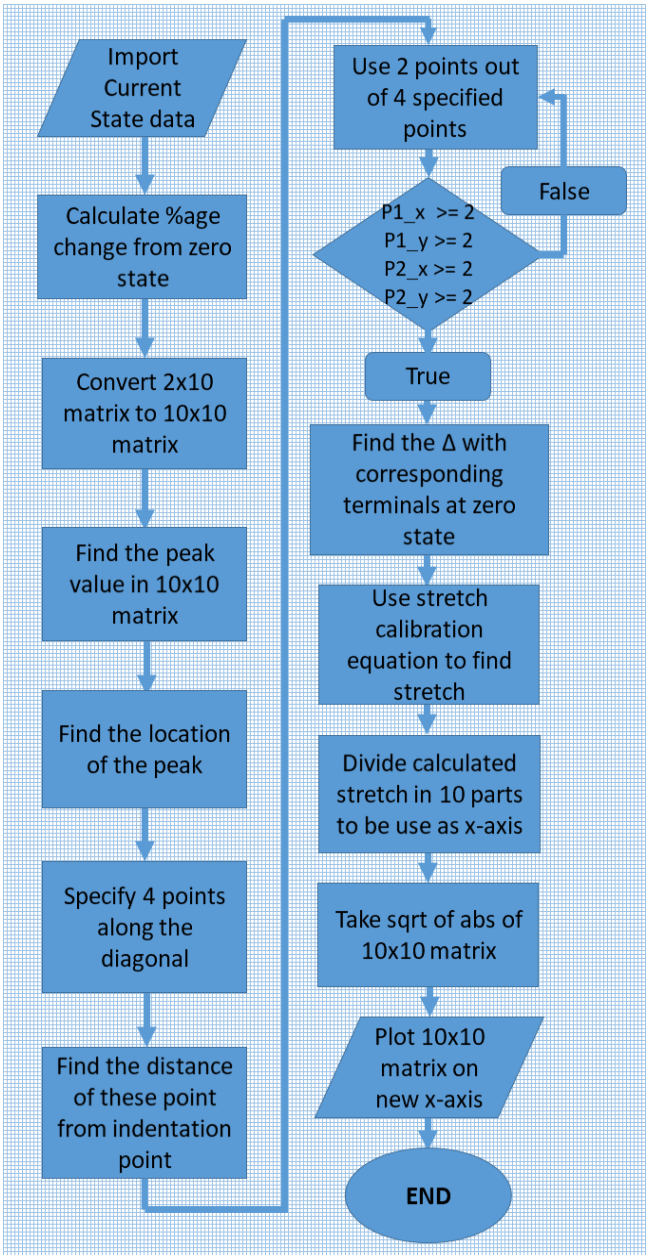

Figure 8: Flow chart of MATLAB algorithm used for decoupling indentation and stretch.

IV. Results and Discussion

First, our algorithm was used on the data for indentations at a stretch 1. The location of the indenter was at node (6,6). The indentation was done in two steps, i.e., at 5mm and then 10mm indentation, and the stretch calculated by the algorithm was 1.0151 and 1.0122. The output of the algorithm is shown in Fig. 9 and Fig. 10. In these figures, the stretch axis is the y-axis along which stretch was applied. As shown in the flowchart, the stretch was calculated and was used to plot deformation, as shown in Fig. 9- 13.

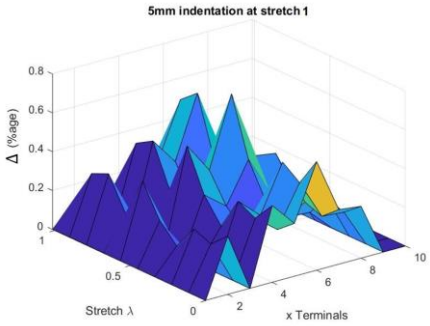

Figure 9: 5 mm indentation at node (6,6) when applied stretch is 1.

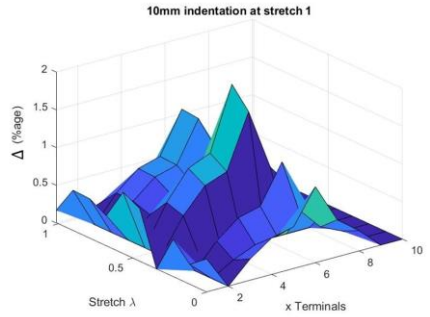

Figure 10: 10 mm indentation at node (6,6) when applied stretch is 1.

Next, the SCEEP was stretched to 1.124 and 1.2475, respectively, and indentations were made at the same node, i.e. (6, 6), Figs. 11 and 12. For applied stretch = 1.124, the stretch calculated by our algorithm with an applied indentation of 5mm was 1.1124, similarly, for an applied stretch = 1.2475, the calculated stretch at 5mm indentation was 1.2381. Fig. 13 shows the change of surface plot when 10mm indentation was applied at node (3,8).

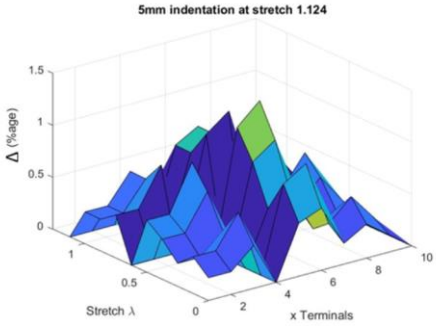

Figure 11: Surface plot of Δ with 5 mm indentation at node (6,6). The applied stretch=1.124; the calculated stretch=1.1124 as shown on stretch axis.

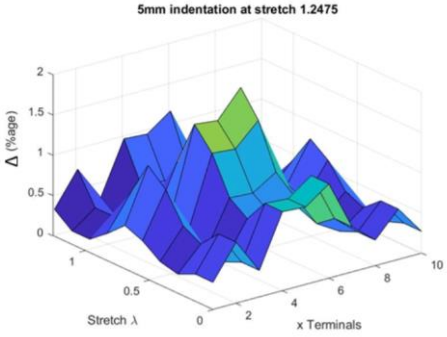

Figure 12: Surface plot of Δ with 5 mm indentation at node (6,6). The applied stretch=1.2475; the calculated stretch=1.2381as shown on stretch axis.

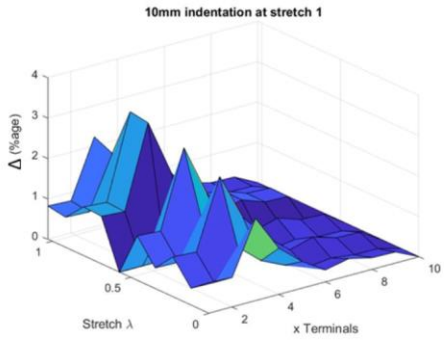

Figure 13: This graph shows the surface plot when a 10 mm indentation is applied at (3,8) and stretch = 1.

It is evident from Figs. 9-12 that for a particular indentation, the Δ capacitance change increases with stretch. This is because, at higher stretches, the local deformation for a particular indentation is larger than at lower stretches. Fig. 14 shows true stretch versus calculated stretch. This plot shows that irrespective of indentation, the algorithm calculated the stretch accurately.

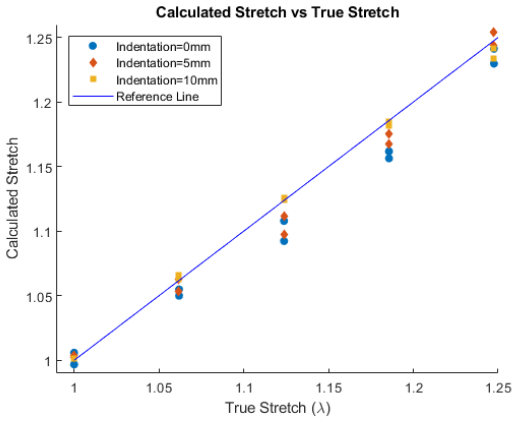

Figure 14: Shows the scatter plot of the calculated stretch from the developed algorithm, against the true stretch. For each particular indentation and stretch, each experiment was repeated twice.

Fig. 15 shows that as the indentation depth is increased, Δ increases at a decreasing rate. Marked trends for the change of capacitance with increasing indentation depth showcase the possibility of being able to quantify the indentation depth from the sensor readings, which we will investigate in the future.

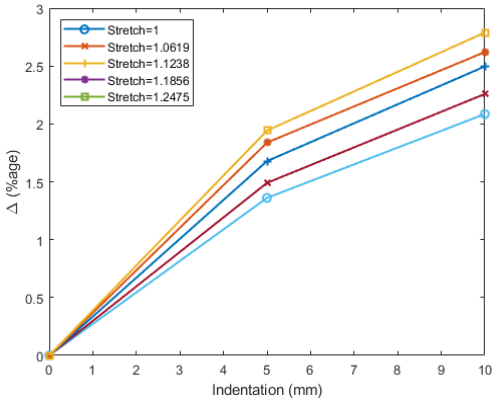

Figure 15: The percentage change in capacitance versus indentation depth; the graph shows Δ with indentations at 5 and 10mm at different stretch levels.

V. Conclusions

In this paper, we have developed a soft capacitive sensing skin and a decoupling algorithm that can be applied to the capacitive readings from 100 tactels and calculate the global strain and identify the location of a local indentation. We fabricated the silicone capacitive skin with three layers of complaint electrodes enclosed in between silicone layers. SCEEP experiences a change in capacitance of all terminals when stretched and a local change in capacitance of only the corresponding terminals when indented in a small region. We developed an algorithm that decouples stretch from indentation. Our algorithm detects the peak of the capacitance change matrix and applies a decision-making approach to determine terminals to be used for calculating stretch. By calculating the percentage change in the capacitance of the selected terminals from their initial state, the stretch is determined. We have achieved an excellent prediction of the global stretch with a maximum error of 2.6% observed in the investigated cases. The results show much promise for combined sensing of different mechanical stimuli which is vital for soft robots interacting with the environment. Future work will use machine learning techniques to improve exteroception and proprioception capabilities using soft sensing skins, and their integration with soft robots.

References

[1] H. Godaba, J. Li, Y. Wang, and J. Zhu, "A Soft Jellyfish Robot Driven by a Dielectric Elastomer Actuator," *IEEE Robot. Autom. Lett.*, vol. 1, no. 2, pp. 624–631, 2016, doi: 10.1109/LRA.2016.2522498.

[2] A. Shiva, A. Stilli, Y. Noh, A. Faragasso, I. De Falco, G. Gerboni, M. Cianchetti, A. Menciassi, K. Althoefer, and H. A. Wurdemann, "Tendon-Based Stiffening for a Pneumatically Actuated Soft Manipulator," *IEEE Robot. Autom. Lett.*, vol. 1, no. 2, pp. 632–637, 2016, doi: 10.1109/LRA.2016.2523120.

[3] C. Lucarotti, M. Totaro, A. Sadeghi, B. Mazzolai, and L. Beccai, "Revealing bending and force in a soft body through a plant root inspired approach," *Sci. Rep.*, p. 8788, 2015, doi: 10.1038/srep08788.

[4] H. Wang, M. Totaro, and L. Beccai, "Toward perceptive soft robots: Progress and challenges," *Adv. Sci.*, vol. 5, no. 9, p. 1800541, 2018.

[5] C. Larson, B. Peele, S. Li, S. Robinson, M. Totaro, L. Beccai, B. Mazzolai, and R. Shepherd, "Highly stretchable electroluminescent skin for optical signaling and tactile sensing," *Science (80-.).*, vol. 351, no. 6277, pp. 1071 LP – 1074, Mar. 2016, doi: 10.1126/science.aac5082.

[6] S. Y. Kim, S. Park, H. W. Park, D. H. Park, Y. Jeong, and D. H. Kim, "Highly Sensitive and Multimodal All-Carbon Skin Sensors Capable of Simultaneously Detecting Tactile and Biological Stimuli," *Adv. Mater.*, vol. 27, no. 28, pp. 4178–4185, 2015, doi: 10.1002/adma.201501408.

[7] H. Xie, H. Liu, S. Luo, L. D. Seneviratne, and K. Althoefer, "Fiber optics tactile array probe for tissue palpation during minimally invasive surgery," in *2013 IEEE/RSJ International Conference on Intelligent Robots and Systems*, 2013, pp. 2539–2544, doi: 10.1109/IROS.2013.6696714.

[8] T. C. Searle, K. Althoefer, L. Seneviratne, and H. Liu, "An optical curvature sensor for flexible manipulators," in *Proceedings - IEEE International Conference on Robotics and Automation*, 2013, pp. 4415–4420, doi: 10.1109/ICRA.2013.6631203.

[9] S. Russo, T. Ranzani, H. Liu, S. Nefti-Meziani, K. Althoefer, and A. Menciassi, "Soft and Stretchable Sensor Using Biocompatible Electrodes and Liquid for Medical Applications," *Soft Robot.*, vol. 2, no. 4, pp. 146–154, Dec. 2015, doi: 10.1089/soro.2015.0011.

[10] J. Park, Y. Lee, J. Hong, M. Ha, Y. Do Jung, H. Lim, S. Y. Kim, and H. Ko, "Giant tunneling piezoresistance of composite elastomers with interlocked microdome arrays for ultrasensitive and multimodal electronic skins," *ACS Nano*, vol. 8, no. 5, pp. 4689–4697, 2014, doi: 10.1021/nn500441k.

[11] T. Wang, Y. Zhang, Q. Liu, W. Cheng, X. Wang, L. Pan, B. Xu, and H. Xu, "A Self-Healable, Highly Stretchable, and Solution Processable Conductive Polymer Composite for Ultrasensitive Strain and Pressure Sensing," *Adv. Funct. Mater.*, vol. 28, no. 7, p. 1705551, 2018, doi: 10.1002/adfm.201705551.

[12] M. Totaro, A. Mondini, A. Bellacicca, P. Milani, and L. Beccai, "Integrated Simultaneous Detection of Tactile and Bending Cues for Soft Robotics," *Soft Robot.*, vol. 4, no. 4, pp. 400–410, 2017, doi: 10.1089/soro.2016.0049.

[13] T. P. Tomo, M. Regoli, A. Schmitz, L. Natale, H. Kristanto, S. Somlor, L. Jamone, G. Metta, and S. Sugano, "A New Silicone Structure for uSkin - A Soft, Distributed, Digital 3-Axis Skin Sensor and Its Integration on the Humanoid Robot iCub," *IEEE Robot. Autom. Lett.*, vol. 3, no. 3, pp. 2584–2591, 2018, doi: 10.1109/LRA.2018.2812915.

[14] T. P. Tomo, A. Schmitz, W. K. Wong, H. Kristanto, S. Somlor, J. Hwang, L. Jamone, and S. Sugano, "Covering a Robot Fingertip with uSkin: A Soft Electronic Skin with Distributed 3-Axis Force Sensitive Elements for Robot Hands," *IEEE Robot. Autom. Lett.*, vol. 3, no. 1, pp. 124–131, 2018, doi: 10.1109/LRA.2017.2734965.

[15] S. Denei, P. Maiolino, E. Baglini, and G. Cannata, "Development of an Integrated Tactile Sensor System for Clothes Manipulation and Classification Using Industrial Grippers," *IEEE Sens. J.*, vol. 17, no. 19, pp. 6385–6396, 2017, doi: 10.1109/JSEN.2017.2743065.

[16] T. Matsuno, Z. Wang, K. Althoefer, and S. Hirai, "Adaptive update of reference capacitances in conductive fabric based robotic skin," *IEEE Robot. Autom. Lett.*, vol. 4, no. 2, pp. 2212–2219, 2019, doi: 10.1109/LRA.2019.2901991.

[17] P. Maiolino, A. Ascia, M. Maggiali, L. Natale, G. Cannata, and G. Mett, "Large Scale Capacitive Skin for Robots," in *Smart Actuation and Sensing Systems - Recent Advances and Future Challenges*, 2012, p. 16.

[18] P. Maiolino, M. Maggiali, G. Cannata, G. Metta, and L. Natale, "A flexible and robust large scale capacitive tactile system for robots," *IEEE Sens. J.*, vol. 13, no. 10, pp. 3910–3917, 2013, doi: 10.1109/JSEN.2013.2258149.

[19] D. H. Ho, Q. Sun, S. Y. Kim, J. T. Han, D. H. Kim, and J. H. Cho, "Stretchable and Multimodal All Graphene Electronic Skin," *Adv. Mater.*, vol. 28, no. 13, pp. 2601–2608, 2016, doi: 10.1002/adma.201505739.

[20] Q. Hua, J. Sun, H. Liu, R. Bao, R. Yu, J. Zhai, C. Pan, and Z. L. Wang, "Skin-inspired highly stretchable and conformable matrix networks for multifunctional sensing," *Nat. Commun.*, vol. 9, no. 1, pp. 1–11, 2018, doi: 10.1038/s41467-017-02685-9.

[21] V. Wall, G. Zöller, and O. Brock, "A method for sensorizing soft actuators and its application to the RBO hand 2," in *2017 IEEE International Conference on Robotics and Automation (ICRA)*, 2017, pp. 4965–4970, doi: 10.1109/ICRA.2017.7989577.

[22] G. Zöller, V. Wall, and O. Brock, "Acoustic Sensing for Soft Pneumatic Actuators," in *IEEE International Conference on Intelligent Robots and Systems*, 2018, pp. 6986–6991, doi: 10.1109/IROS.2018.8594396.

[23] U. Culha, S. G. Nurzaman, F. Clemens, and F. Iida, "SVAS3: Strain vector aided sensorization of soft structures," *Sensors (Switzerland)*, vol. 14, no. 7, pp. 12748–12770, 2014, doi: 10.3390/s140712748.

[24] A. Iggo, "Cutaneous Receptors," in *The Peripheral Nervous System*, In: Hubbard J.I. (eds), Ed. Springer, Boston, MA, 1974, pp. 347–404.

[25] A. B. Dawood, H. Godaba, and K. Althoefer, "Modelling of a soft sensor for exteroception and proprioception in a pneumatically actuated soft robot," in *Lecture Notes in Computer Science*, 2019, vol. 11650 LNAI, pp. 99–110, doi: 10.1007/978-3-030-25332-5_9.

[26] J. Lee, M. T. Cole, J. C. S. Lai, and A. Nathan, "An analysis of electrode patterns in capacitive touch screen panels," *IEEE/OSA J. Disp. Technol.*, vol. 10, no. 5, pp. 362–366, 2014, doi: 10.1109/JDT.2014.2303980.